

## Electronic structure of the actinide-Rh<sub>3</sub> systems and the 5*f* localization in UPd<sub>3</sub>

Olle Eriksson\* and Börje Johansson

*Condensed Matter Theory Group, Institute of Physics, University of Uppsala, P.O. Box 530, S-751 21 Uppsala, Sweden*

M. S. S. Brooks

*European Institute for Transuranium Elements, Commission of the European Communities, Joint Research Centre, P.O. Box 2340, D-7500 Karlsruhe, Federal Republic of Germany*  
*and Condensed Matter Theory Group, Institute of Physics, University of Uppsala, P.O. Box 530, S-751 21 Uppsala, Sweden*

H. L. Skriver

*Laboratory of Applied Physics, Technical University of Denmark, DK-2800 Lyngby, Denmark*

(Received 4 April 1989)

We present electronic-structure calculations for the isostructural (AuCu<sub>3</sub>-structure) series of intermetallic compounds  $ARh_3$  ( $A = \text{Ac, Th, Pa, U, Np, Pu, Am, and Cm}$ ). The calculations were performed using both the scalar relativistic and the fully relativistic linear muffin-tin orbital (LMTO) method. Calculated cohesive and magnetic properties are compared with available experimental data. The onset of magnetism is discussed by means of a relativistic Stoner theory. The influence of the ligand states on the uranium 5*f* electrons is studied for the  $UM_3$  ( $M = \text{Mo, Tc, Ru, Rh, Pd, and Ag}$ ) series of compounds. The localization of the 5*f* electrons in UPd<sub>3</sub> as opposed to the itinerant 5*f* behavior for the earlier compounds (UMo<sub>3</sub>, UTc<sub>3</sub>, URu<sub>3</sub>, and URh<sub>3</sub>) is explained in terms of the variation of the hybridization between 5*f* and ligand 4*d* states through the series.

### I. INTRODUCTION

In the last few years a lot of attention has been paid to the basic electronic structure of actinide (*A*) materials. One important problem in these investigations<sup>1</sup> has concerned the nature of the 5*f* electrons, namely whether they are localized like the 4*f* electrons generally are in corresponding lanthanide systems, or if they are itinerant and actively contribute to the chemical bonding<sup>2</sup> like the *d* electrons<sup>3</sup> in the 3*d*, 4*d*, and 5*d* transition metals. For the actinide metals there are now strong experimental and theoretical evidences available for a sharp change of the 5*f* behavior between Pu and Am, namely that the 5*f* electrons are itinerant for the early actinides and localized, rare-earth-like for the heavier elements.<sup>4</sup> This gives, for example, rise to a dramatic increase of the equilibrium atomic volume when proceeding from Pu to Am, the difference being about 8 Å<sup>3</sup> which is an increase of 40%. Thus the question about localized versus itinerant 5*f* behavior is far from being just an academic question but has most important consequences for bulk properties of the material. The atomic volumes of the actinide metals including the dramatic rise between Pu and Am have been well explained by theory.<sup>4</sup>

For actinide compounds the situation concerning the nature of the 5*f* electrons is presently less clear. Furthermore it might be that the difference between local and itinerant 5*f* behavior is not as distinct in compounds as it appears to be for the pure elements. The existence and properties of the heavy-fermion superconductors seem to indicate that the delocalization under certain circumstances might appear to be gradual rather than

sharp.<sup>5</sup> Therefore in the study of the electronic structure of actinide systems it is important to clarify for which type of materials a conventional band-structure approach is applicable for the 5*f* electrons, i.e., when they are fully itinerant. When the band approach fails it is also useful to investigate to what extent and in which respect it fails.

Among actinide intermetallic compounds the  $ARh_3$  systems form an attractive class of materials to study since they are isostructural (AuCu<sub>3</sub> cubic structure). Of special interest is the fact that as a function of the actinide atomic number there is a quite dramatic increase of the molar volume between PuRh<sub>3</sub> and AmRh<sub>3</sub>. This increase is in fact similar to the one for the pure elements, and it becomes tempting to associate this with an effect of 5*f* localization. Apparently this localization of the 5*f* electrons as a function of increasing atomic number should mainly originate from the contraction of the 5*f* orbitals and the increasing number of 5*f* electrons. However, the immediate atomic neighborhood to the actinide atoms in the crystal is also of great importance for the 5*f* behavior.<sup>6</sup>

For a study of the effect of a ligand on the nature of the 5*f* electrons experimental evidence suggests that an investigation of the  $UM_3(4d)$  intermetallic systems as a function of the 4*d* transition element ( $M = {}_{42}\text{Mo}, {}_{43}\text{Tc}, \dots, {}_{47}\text{Ag}$ ) should be most revealing. As a complementary study of the 5*f* behavior as a function of the actinide element *A* for a given ligand ( $ARh_3$ ), we therefore investigate the property of the 5*f* electrons for a fixed actinide element but as a function of the ligand *M* [ $UM_3(4d)$ ]. For this latter series of compounds there are experimental data available which suggest an itinerant 5*f*

behavior in URh<sub>3</sub> (Ref. 7) and a localized one in UPd<sub>3</sub>.<sup>8</sup> This means that for this class of uranium systems a 5*f* localization takes place as a function of the ligand atomic number. It is however somewhat unfortunate that the URh<sub>3</sub> and UPd<sub>3</sub> systems have different crystal structures. Thus URh<sub>3</sub> has the AuCu<sub>3</sub> cubic structure while UPd<sub>3</sub> has the hexagonal TiNi<sub>3</sub> structure. Still it seems unlikely that this difference in structure should be the decisive factor for the difference in the 5*f* behavior, but that the main effect should originate from the change of the ligand. If the difference in structure should turn out to depend on the nature of the 5*f* electrons, then it is still likely that this crystallographic change should only be a second-order effect. The fact that ZrRh<sub>3</sub> and ZrPd<sub>3</sub> show the same crystal-structure change<sup>9</sup> as URh<sub>3</sub> and UPd<sub>3</sub> provides strong evidence that the 5*f* electrons are at most of secondary importance for the structure.

In the present work we will present electronic structure calculations for the two mentioned classes of materials. It is a great advantage to be able to study a whole class of systems since thereby the gradual changes from one system to another can be followed and possible systematic errors in the theoretical treatment will tend to cancel. This also helps in the identification of the important factors which are decisive for the behavior of the physical properties. In Sec. II we present paramagnetic and spin-polarized scalar relativistic calculations for the ARh<sub>3</sub> systems and discuss the volume change upon the formation of the compounds. A simplified model for the electronic structure of the ARh<sub>3</sub> compounds is introduced in Sec. III. Fully relativistic calculations are presented in Sec. IV and a relativistic version of the Stoner criterion for ferromagnetism is outlined in Sec. V. Calculations for the UM<sub>3</sub> (*M* = <sub>42</sub>Mo, <sub>43</sub>Tc, . . . , <sub>47</sub>Ag) systems are discussed in Sec. VI. Section VII contains some concluding remarks.

## II. RESULTS

The calculations were done using the linear muffin-tin orbital (LMTO) method with the inclusion of the so-called combined correction terms.<sup>10</sup> In the calculation of the self-consistent valence charge density the irreducible wedge of the Brillouin zone was sampled at 35, 56, and finally 120 *k* points. Furthermore the frozen-core approximation was used together with the von Barth-Hedin parameterization<sup>11</sup> of the exchange and correlation potential. Finally the density of states (DOS) was calculated by using the analytical tetrahedron method.<sup>12</sup>

The experimental and calculated equilibrium formula unit volumes for the ARh<sub>3</sub> systems are plotted in Fig. 1. The theoretical data were obtained from three different types of approaches: a scalar relativistic, a spin-polarized scalar relativistic, and a fully relativistic calculation, where only the first two will be discussed in this section. We notice that for the scalar relativistic calculation the trend of the lattice constants is similar to that of the pure actinide elements and that for the earlier compounds in the series theory reproduces the experimental data well. This suggests that the band picture of the 5*f* states pro-

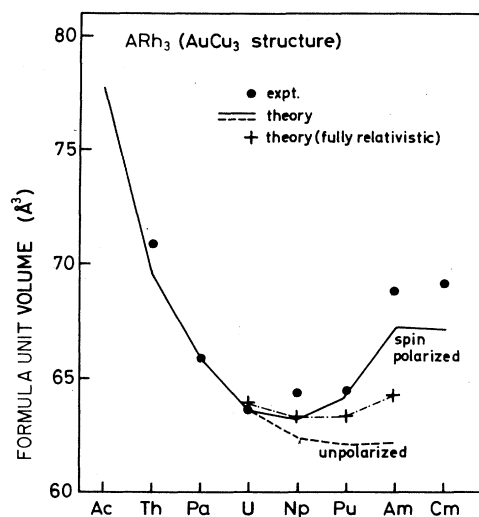


FIG. 1. Experimental as well as calculated formula unit volumes for the ARh<sub>3</sub> systems. The calculated volumes have been obtained from several different types of calculations. The volumes from the paramagnetic scalar relativistic calculations are drawn as a solid line for Ac-U and a dashed line for Np-Am, whereas the volumes from the scalar relativistic spin-polarized calculations are marked with a solid line for Np-Cm. The volumes from a fully relativistic calculation are marked with crosses that are connected with a dashed line.

vides an adequate description of their electronic structure.

For the heavier compounds shown in Fig. 1 it is known from experiments that between PuRh<sub>3</sub> and AmRh<sub>3</sub> there is a jump in the lattice constants that corresponds to a change of the formula unit volume of 4.4 Å<sup>3</sup>. This is considerably smaller than the atomic volume change between the Pu and Am metals, where it is about 8 Å<sup>3</sup>. As already mentioned, the change of volume between Pu and Am has been shown to originate from the lack of 5*f* bonding in Am as opposed to Pu where the 5*f* electrons contribute to the metallic cohesion.<sup>2,4</sup> Similarly, the abrupt change of the lattice constant between PuRh<sub>3</sub> and AmRh<sub>3</sub> also seems to indicate that the 5*f* electrons are localized in AmRh<sub>3</sub>. Furthermore the good agreement above between the experimental and theoretical (with the 5*f* electrons treated as itinerant) lattice constants for the early ARh<sub>3</sub> compounds strongly suggests that the 5*f* electrons are delocalized and take part in the bonding. However, if the 5*f* electrons are considered as localized in AmRh<sub>3</sub>, then the comparatively small jump in the lattice constant between PuRh<sub>3</sub> and AmRh<sub>3</sub> seems anomalous. One purpose of the present work is to explain the cause of this anomaly.

First, however, we shall need to study in more detail the physical factors that give rise to the parabolic trend in the lattice constants for the early ARh<sub>3</sub> systems. Just as for the actinide metals our present calculations show that for the early ARh<sub>3</sub> systems the 5*f* electrons are delocalized and strongly contribute to the chemical bonding. These delocalized 5*f* states are progressively filled as we proceed from one compound to another through the series. This is illustrated in Fig. 2, where we have plotted

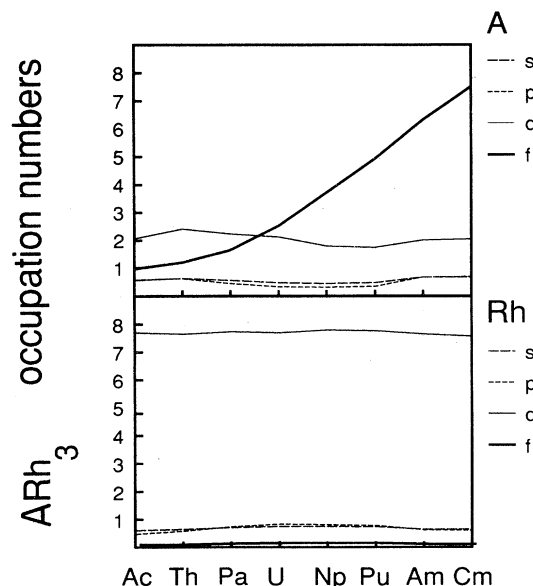


FIG. 2. Calculated partial occupation numbers for the  $ARh_3$  systems.

the partial occupation numbers of the various orbitals, and we notice that the number of  $5f$  electrons increases by approximately one, when the nuclear charge increases by one. The other partial occupation numbers remain more or less constant through the series. This indicates that the major changes of the different contributions to the chemical bonding are to be found from the  $5f$  electrons.

It has been shown that the partial electronic pressure  $p_l$  from the  $l$ th orbital can be approximated by the following transparent expression:<sup>10,13</sup>

$$3p_l V = n_l (-\partial C_l / \partial \ln S) + n_l (\bar{E}_l - C_l) (\partial \ln W_l / \partial \ln S). \quad (1)$$

Here  $\bar{E}_l$  is the center of gravity of the occupied part,  $C_l$  is the center,  $W_l$  the bandwidth, and  $n_l$  is the occupation number of the  $l$ th orbital. The quantities  $V$  and  $S$  are the volume and radius of the Wigner-Seitz cell, respectively. The derivatives  $\partial C_l / \partial \ln S$  and  $\partial \ln W_l / \partial \ln S$  can be calculated from the radial wave equation. Equation (1) shows that the electronic pressure can be divided into two terms, the first is called the band-center term and the second is called the bandwidth term. These two approximate contributions to the  $5f$  pressure in the  $ARh_3$  series have been plotted in Fig. 3(a), together with their sum. Also the total  $5f$  pressure obtained from the full band calculations is shown. Figures 3(b) and 3(c) illustrate the partial pressures, obtained from the full calculations, for all the partial waves. We notice here that, at the experimental volume, the  $5f$  partial pressure is bonding (negative) and has a parabolic behavior through the series. The other partial pressures for the actinide-atom remain more or less constant, with the actinide  $d$  electrons having a negative contribution and the actinide  $sp$  electrons having a positive contribution to the pressure. The par-

tial pressure is also positive for the Rh  $sp$  electrons, whereas the Rh  $d$  partial pressure is negative and almost constant through the series. The results from Eq. (1) show that the  $5f$  band-center term is quite small, positive, and practically constant for the different compounds and that the  $5f$  bandwidth term is large and negative, and shows a parabolic type of behavior [Fig. 3(a)]. This is due to the fact that the bandwidth term in Eq. (1) depends on the product of the  $5f$  occupation number (which increases approximately linearly with atomic number) and the  $(\bar{E}_l - C_l)$  term (which decreases almost linearly with atomic number). Since  $\partial \ln W_l / \partial \ln S$  is practically constant the net result is then a parabolic trend of the  $5f$  partial pressure as a function of the atomic number and this affects the equilibrium volumes correspondingly.

We will now discuss the reasons for the relatively small change in the molar volume between  $PuRh_3$  and  $AmRh_3$ . In Fig. 4 we plot the difference between the experimental

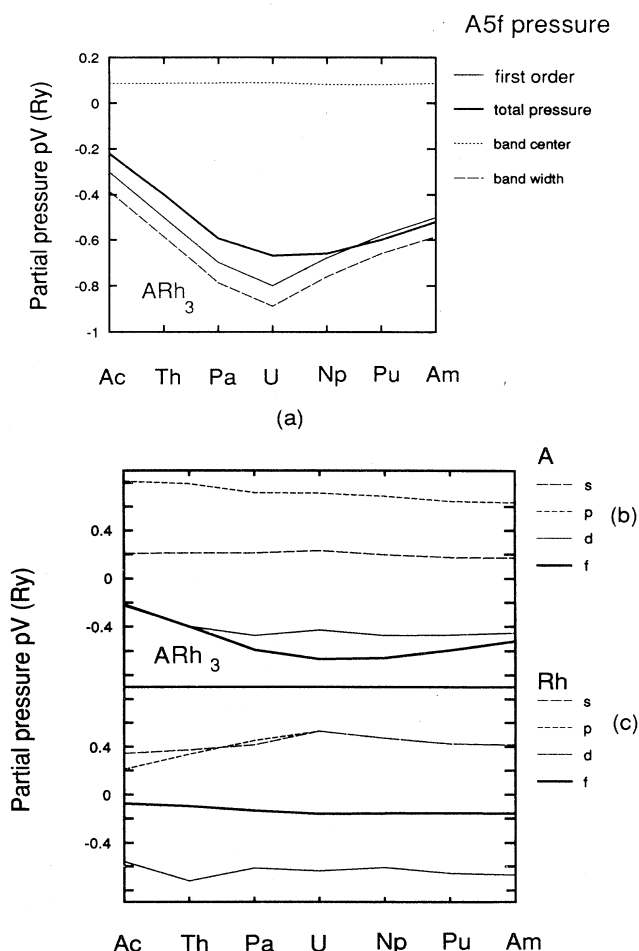


FIG. 3. (a) Electronic  $5f$  partial pressure calculated from Pettifor's pressure formula and from the first-order pressure relation [Eq. (1)]. The first-order pressure has been divided into its two components, the bandwidth and band-center term. (b) Partial electronic pressure for the actinide- $s$ ,  $p$ ,  $d$ , and  $f$  states in the  $ARh_3$  systems. (c) Partial electronic pressure for the Rh  $s$ ,  $p$ ,  $d$ , and  $f$  states in the  $ARh_3$  systems.

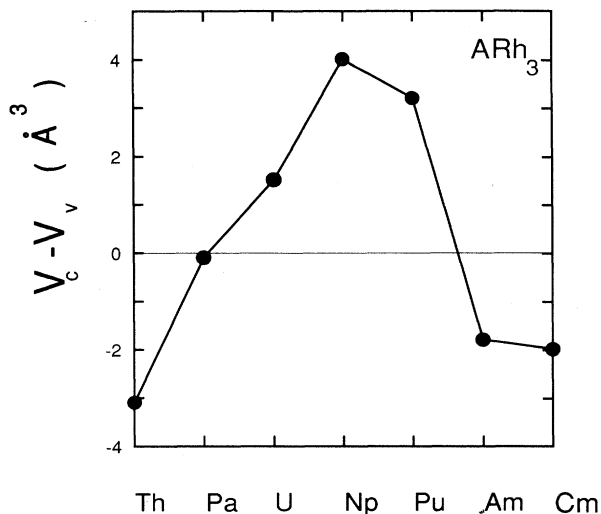


FIG. 4. Deviation from Vegard's law for the  $ARh_3$  systems, i.e., the difference between the volume of the specific compound  $V_c$  and the volume estimated from Vegard's law  $V_v$ .

formula unit volumes and the volumes obtained from Vegard's law<sup>14</sup> (where the volume is derived from the sum of the atomic volumes of the individual elements with appropriate weight factors),

$$\Delta V = V_{\text{compound}} - V_{\text{Vegard}} \quad (2)$$

It is clear from Fig. 4 that  $\Delta V$  is negative for the compounds where we expect the  $5f$  contribution to the chemical bonding to be negligible both in the pure metal state and in the compound (Th, Am, and Cm). A negative  $\Delta V$  is usually associated with the compound formation itself, namely that the bonding in the compound is larger than in the individual elements that form the compound, hence the contraction. For the systems with delocalized bonding  $5f$  electrons, however, the data shows that  $\Delta V$  is positive. In order to relate the compounds with non-bonding  $5f$  electrons to similar systems, we show in Fig. 5 the experimental and calculated volumes for a number

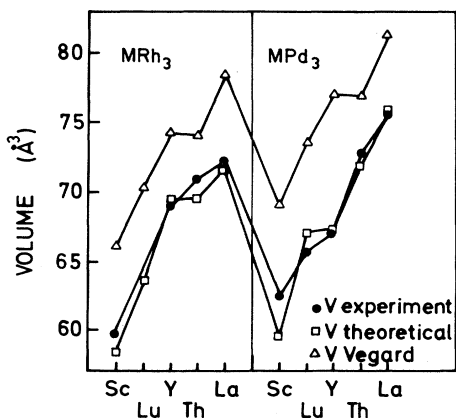


FIG. 5. Experimental and theoretical formula unit volumes for the  $MRh_3$  and  $MPd_3$  systems ( $M = {}_{21}\text{Sc}$ ,  ${}_{39}\text{Y}$ ,  ${}_{72}\text{Lu}$ ,  ${}_{90}\text{Th}$ , and  ${}_{57}\text{La}$ ). Also given are the volumes obtained from Vegard's law for these systems.

of  $AuCu_3$  compounds involving early and late  $d$  transition elements. In this figure we have also plotted the volumes Vegard's law would predict for these compounds. In all cases the simple Vegard's law overestimates the volume, whereas our theoretical calculations in general agree quite well with experiment. The reason for the large contractions in these compounds is to be found in the unusually strong stability of intermetallic compounds between an early and a late  $d$  transition element.<sup>15,16</sup>

The mentioned stability for compounds between early and late  $d$  transition elements can be understood in rather simple terms. To illustrate the prominent features of the electronic structure change upon compound formation we simplify by considering only the  $d$  density of states (DOS), which in fact gives the dominant contribution to the bonding. It is important to notice that for an early transition element the  $d$  level is considerably higher in energy than for a late transition element. In Fig. 6(a) we show a schematized form of the DOS for the two separated metals. For the early transition metal we have a low filling of the  $d$  DOS and for the late transition metal an almost filled  $d$  DOS. When the elements are brought together to form a compound, the  $d$  orbitals of the two elements start to hybridize with each other. Then the total DOS of the combined system takes the simplified form illustrated in Fig. 6(b), which could be classified as composed of a bonding and antibonding part. Compared to the two separated metals in Fig. 6(a), considerable energy has been gained in the formation of the intermetallic system. The bonding part of the DOS to the right in Fig. 6(b) is composed of a strong hybrid between the  $d$  levels of the early and late transition element. Hence the filling of the bonding band takes place with no or little charge transfer.

The gain in bonding energy upon formation of the compound is also associated with contracted volumes. Thus the large energy gain in the formation of an intermetallic compound between late and early transition

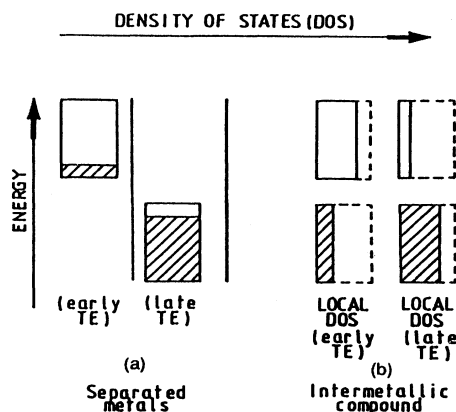


FIG. 6. (a) Schematic density of states for two separated early and late transition metals ( $d$  bands only). The occupied part in each band is hatched. (b) Schematic density of states for two hybridizing  $d$  states between an early and late transition metal forming a compound. The occupied states are denoted with hatched areas.

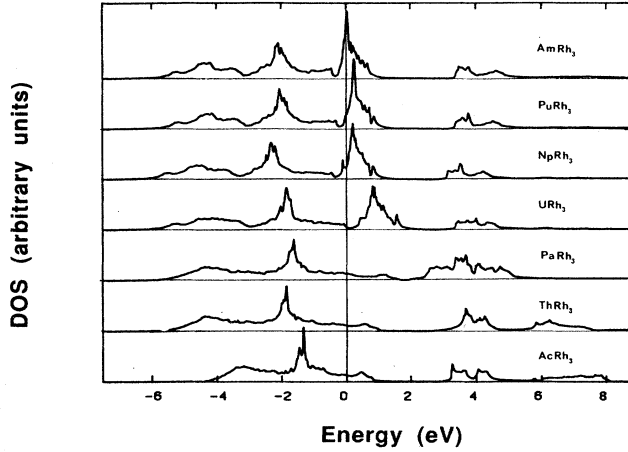


FIG. 7. Paramagnetic scalar relativistic density of states for the  $ARh_3$  systems at the experimental volume for each compound. The Fermi level is at zero energy.

metals explains why Vegard's law overestimates the equilibrium volume. The same picture will also be valid for compounds between  $f$  transition elements and late  $d$  transition elements, when the  $f$  electrons are nonbonding both in the elemental metal and in the corresponding compounds. However for  $URh_3$ ,  $NpRh_3$ , and  $PuRh_3$  the situation is different as revealed by the volume expansion upon formation of the compound. A similar situation is also met with for the  $AIr_2$  compounds ( $A = {}_{92}U, {}_{93}Np, {}_{94}Pu$ ). This has recently been shown to be caused by a decrease of  $5f$  bonding, due to band narrowing, in the intermetallic  $AIr_2$ -systems relative to the pure metals.<sup>17</sup> In the present case of the  $ARh_3$  systems we find that the  $5f$  band widths are reduced to about 0.7 of the bandwidths in the pure metals. This reduction is similar to that for the  $AIr_2$  compounds and causes a reduction of the  $5f$  bonding.

Hence there are two competing effects, namely gain of

$d$  bonding and loss of  $f$  bonding in the formation of the compound relative to its constituents. To a large extent they seem to cancel each other out in  $PaRh_3$  (which has only one  $5f$  electron), since here Vegard's law apparently is obeyed (Fig. 4). For the following compounds  $URh_3$ ,  $NpRh_3$  and  $PuRh_3$  the loss of  $f$  bonding is more prominent and gives rise to a positive deviation from Vegard's law. This will also be reflected in the heats of formation of these compounds which will be correspondingly reduced relative to compounds involving non- $f$  transition metals. For the localized  $f$  system  $AmRh_3$ , there is no loss of  $f$  bonding in the formation of the compound. Therefore the loss of  $f$  bonding for  $PuRh_3$  relative to  $Pu$  metal will give rise to a smaller volume difference between  $PuRh_3$  and  $AmRh_3$  than between  $Pu$  and  $Am$ . This shows that a possible explanation of the volume change between  $PuRh_3$  and  $AmRh_3$  could be associated with  $f$  localization in  $AmRh_3$  and that due to the above-mentioned effects the volume difference will be smaller for the compounds than for the pure metals. Another possible explanation of the change in volumes between  $PuRh_3$  and  $AmRh_3$  is that the  $5f$  electrons are localized in  $PuRh_3$  with a tetravalent  $5f^4$  configuration, while  $Am$  has a trivalent  $5f^6$  configuration in  $AmRh_3$ . This localized picture for  $PuRh_3$  is given some support from the fact that the magnetic entropy in  $PuRh_3$  is of the order  $R \ln 2$ .<sup>18</sup>

### III. ELECTRONIC STRUCTURE

The calculated paramagnetic scalar relativistic electron density of states for the  $ARh_3$  systems is shown in Fig. 7. Here we notice that the bonding and antibonding  $d$  states are well separated in energy, just as illustrated schematically in Fig. 6. For  $URh_3$ ,  $NpRh_3$ ,  $PuRh_3$ , and  $AmRh_3$  the actinide  $5f$  resonance essentially lies at the upper part of the bonding band and hybridizes strongly with it. This hybridization is crucial for the formation of the  $5f$  bands in these systems and one way to illustrate this is to calculate the bandwidth when hybridization is omitted. An estimate of the unhybridized band width (of the  $tl$  band,

TABLE I. Second moments for the different  $tl, t'l'$  blocks in the structure constants for the  $AuCu_3$  lattice. Also given are the parameters  $\Delta_{tl}$  [Eq. (5)],  $W_{tl}^0$  [Eq. (4)] and the difference between the center of bands for the actinide  $5f$ , actinide  $6d$ , and Rh  $4d$  orbitals. The number of  $5f$  states that according to Eq. (5) hybridizes into the Rh  $4d$  band is also given ( $N_{Rh d}^{A f}$ ), as well as the corresponding occupation number [ $N_{Rh d}^{A f}(\text{occ.})$ ].  $|S_{A f}^{A f}|^2 = 2.1$ ,  $|S_{Rh d}^{Rh d}|^2 = 446.7$ ,  $|S_{Rh d}^{A f}|^2 = 286.5$ ,  $|S_{A d}^{A d}|^2 = 3.5$ .

	AcRh <sub>3</sub>	ThRh <sub>3</sub>	PaRh <sub>3</sub>	URh <sub>3</sub>	NpRh <sub>3</sub>	PuRh <sub>3</sub>	AmRh <sub>3</sub>	CmRh <sub>3</sub>
$\Delta_{Rh d}$ (mRy)	18.8	18.7	18.1	18.2	17.6	17.6	18.1	18.2
$\Delta_{A d}$ (mRy)	203	199	144	123	113	116	132	141
$\Delta_{A f}$ (mRy)	149.6	63.2	19.7	13.2	10.5	8.5	5.1	4.1
$W_{Rh d}^0$ (Ry)	0.35	0.35	0.34	0.34	0.33	0.33	0.34	0.34
$W_{A d}^0$ (Ry)	0.588	0.576	0.417	0.356	0.328	0.336	0.383	0.408
$W_{A f}^0$ (Ry)	0.271	0.120	0.039	0.025	0.019	0.015	0.009	0.008
$C_{A d}-C_{Rh d}$ (Ry)	0.502	0.448	0.428	0.482	0.519	0.531	0.425	0.402
$C_{A f}-C_{Rh d}$ (Ry)	1.251	0.746	0.301	0.190	0.164	0.146	0.111	0.110
$N_{Rh d}^{A f}$	1.0	1.2	2.2	3.8	3.9	4.0	4.3	3.7
$N_{Rh d}^{A f}(\text{occ.})$	0.8	1.0	1.7	3.3	3.4	3.5	3.8	3.2

where  $t$  is the atom-type and  $l$  is the orbital character) has been shown to be<sup>19</sup>

$$W_{il}^0 = \left[ \frac{12}{N_{il}} |S_{il}^{tl}|^2 \right]^{1/2} \Delta_{il}, \quad (3)$$

where  $\Delta_{il}$  is given by

$$\Delta_{il} = 1 / [\mu_{il} S_t^2 (S/S_t)^{2l+1}]. \quad (4)$$

The quantity  $|S_{il}^{tl}|^2$  is the second moment of the canonical  $tl$  band and is thus a property only depending on the crystal structure,  $S_t$  is the atomic radius of the  $t$  atom,  $N_{il}$  equals  $n_t(2l+1)$ , where  $n_t$  is the number of  $t$ -type atoms per primitive cell. Furthermore  $S$  is the characteristic radius of the lattice (which is a linear dimension of the lattice,<sup>19</sup> in the present work chosen as the average radius per formula unit) and  $\mu_{il} [= (1/S_t^3 \phi^2(S_t))$ , where  $\phi(S_t)$  is the value of the wave function at the Wigner-Seitz radius] is the band mass. In Table I we show the values of  $|S_{il}^{tl}|^2$ ,  $\Delta_{il}$ , and  $W_{il}$  for the actinide  $f$ , actinide  $d$ , and Rh  $d$  states, for all the  $ARh_3$  systems. Here it is obvious that the unhybridized  $5f$ -band width [given by Eq. (3)] is much smaller than for the fully hybridized band widths in all these systems (Fig. 7). This shows that the hybridization between the actinide  $5f$  states and the ligand states is of overriding importance in these systems. In order to determine which ligand partial wave function that is dominant for this hybridization we calculate the number of actinide  $5f$  electrons that lies in what unhybridized was pure ligand  $s$ ,  $p$ , and  $d$  states. This can be done using the expression,<sup>19</sup>

$$N_{il}^{t'l'} = 2 |S_{il}^{t'l'}|^2 \Delta_{il} \Delta_{t'l'} (C_{il} - C_{t'l'})^{-2}. \quad (5)$$

Here  $|S_{il}^{t'l'}|^2$  is the second moment of the block in the structure constants that connect the  $tl$  and  $t'l'$  bands and  $C_{il}$  is the center of the  $tl$  band. It turns out using Eq. (5) that it is the actinide  $5f$  and ligand  $4d$  hybridization that is by far dominating. The actual values of the number of actinide  $5f$  states that enters into what unhybridized was a  $4d$  band are given in Table I, together with the values of

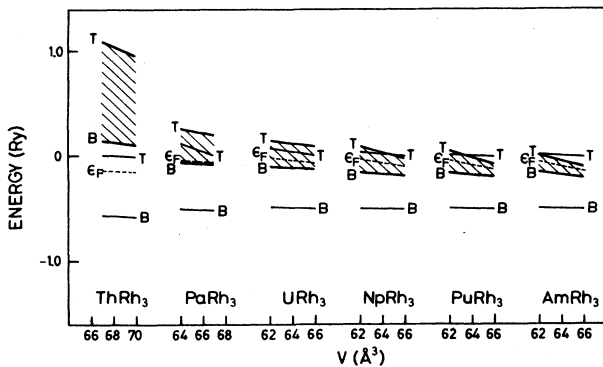


FIG. 8. Schematic picture of the electronic structure for the  $ARh_3$  systems as a function of the formula unit volume  $V$  (for details see text). The actinide  $5f$  states are in the hatched region. The top and the bottom of the Rh  $d$  states are indicated by thin lines.  $B$  is the bottom of each band and  $T$  is the top. The Fermi level is marked with  $E_F$ .

$C_{il} - C_{t'l'}$ . Here we also give the number of occupied actinide  $5f$  electrons residing in the bonding band.

Another way to get an estimate of the band states in metals and compounds is to determine when the radial wave function for a given angular momentum is either zero (which corresponds to the top of the band) or when its derivative is zero (which corresponds to the bottom of the band). This is the Wigner-Seitz rule for band formation.<sup>10</sup> In Fig. 8 we illustrate, using this rule, the position of the actinide  $5f$  states and the Rh  $4d$  states together with the Fermi level  $E_F$  as a function of volume. Here we notice that in  $ThRh_3$  the  $5f$  states lies above  $E_F$  and are essentially unoccupied and quite broad. In  $PaRh_3$  the bottom of the  $5f$  band lies just below  $E_F$  and in this compound the  $5f$  states start to become populated. For the systems  $URh_3$ ,  $NpRh_3$ ,  $PuRh_3$ , and  $AmRh_3$ , we observe that the  $5f$  band becomes increasingly narrow and that  $E_F$  lies within this band. Here we also notice the progressive filling of the  $5f$  band as we move across the series of compounds. On the other hand the Rh  $4d$  states seem to be rather invariant for the present series of compounds.

#### IV. RELATIVISTIC EFFECTS

In Fig. 9 we show the paramagnetic DOS for  $URh_3$ ,  $NpRh_3$ ,  $PuRh_3$ , and  $AmRh_3$  as obtained from the fully relativistic calculations<sup>20</sup> (at a constant volume of  $65 \text{ \AA}^3$ ). These DOS look very much like the scalar relativistic ones in Fig. 7 for all partial waves except the actinide  $f$  states. This is due to the fact that it is only for the  $f$  states that the spin-orbit splitting is large enough to cause any appreciable effect. The  $5f$  states are seen to be split into a  $5f_{5/2}$  and a  $5f_{7/2}$  band, which especially for the heavier compounds become almost entirely separated from each other. The value of the spin-orbit splitting is given in Table II for the studied systems and is found to

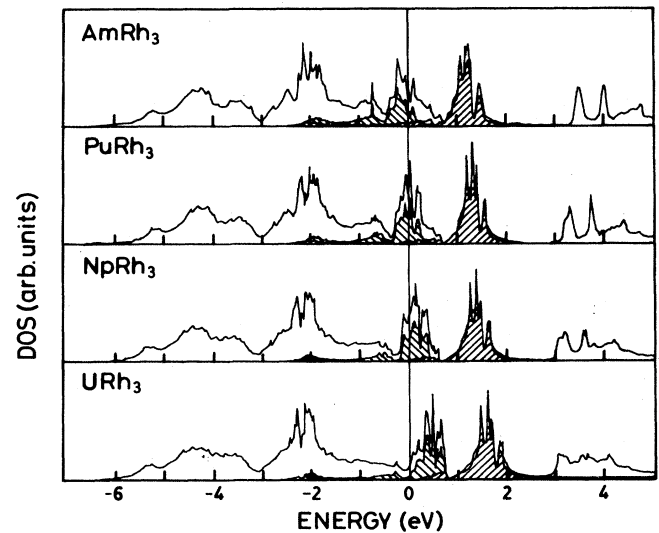


FIG. 9. Fully relativistic density of states for the  $ARh_3$  systems ( $A=U, Np, Pu, \text{ and } Am$ ). The  $5f_{5/2}$  partial density of states is hatched from right to left and the  $5f_{7/2}$  partial density of states from left to right. The Fermi level is at zero energy.

TABLE II. Total density of states (DOS) at the Fermi level from the paramagnetic scalar relativistic calculation is listed as  $D(\text{para})$ . Multiband Stoner product from the same calculation is denoted  $ID(\text{para})$ .  $n_f$  is the total number of  $5f$  electrons obtained from the scalar relativistic calculation whereas the  $j = \frac{5}{2}$  and  $j = \frac{7}{2}$  decomposed occupation numbers from the fully relativistic calculation are given as  $n_{5f_{5/2}}$  and  $n_{5f_{7/2}}$ , respectively. The partial DOS at the Fermi level for the  $j = \frac{5}{2}$  and  $j = \frac{7}{2}$  bands from the fully relativistic calculation are labeled  $D_{5/2}$  and  $D_{7/2}$ , respectively. Also given is the total Rh  $d$  DOS at the Fermi level from this calculation  $D_{\text{Rh}d}$ . Calculated exchange integrals for the Rh  $4d$  and actinide  $5f$  states are denoted  $J_{\text{Rh}d}$  and  $J_{Af}$ , respectively, and the relativistic Stoner product is given as  $ID(\text{rel})$ . (The densities of states are given in units of states/Ry formula-unit.)

	URh <sub>3</sub>	NpRh <sub>3</sub>	PuRh <sub>3</sub>	AmRh <sub>3</sub>
$D(\text{para})$	70	107	260.6	568
$ID(\text{para})$	0.4	0.9	3.5	7.7
$\Delta_{s.o.}$ (eV)	1.3	1.4	1.5	1.6
$n_{5f}$	2.63	3.77	4.93	6.05
$n_{5f_{5/2}}$	1.69	2.81	3.98	5.00
$n_{5f_{7/2}}$	0.94	0.96	0.95	1.05
$D_{5/2}$	5	71	108	62
$D_{7/2}$	1	3	7	9
$D_{\text{Rh}d}$	41	46	59	53
$J_{\text{Rh}d}$ (Ry)	0.036	0.036	0.036	0.036
$J_{Af}$ (Ry)	0.039	0.041	0.039	0.040
$ID(\text{rel})$	0.4	0.7	1.1	0.7

be of similar magnitude to the calculated scalar relativistic  $5f$ -band width. The spin-orbit splitting was calculated as the difference in energy between the  $5f_{5/2}$  and  $5f_{7/2}$  bands when they have the same logarithmic derivative. In this case we evaluated the spin-orbit splitting at the center of the bands, i.e., when the logarithmic derivative is  $-l-1$ . The reason why the spin-orbit splitting is comparatively large as compared to the pure metals is a combined effect between the spin-orbit splitting parameter (which is an atomic property) and the crystal field. For URh<sub>3</sub> the DOS is very similar to that reported earlier by Oguchi *et al.*<sup>21</sup>

Even though the electronic structure is changed quite dramatically by the spin-orbit interaction, integrated properties, such as occupation numbers and partial pressures, do not change very much. In Table II we show the total  $5f$  occupation numbers together with the decomposed  $5f_{5/2}$  and  $5f_{7/2}$  occupations as obtained from the fully relativistic calculation. Here we notice that although the total number of  $5f$  electrons is hardly changed as compared to the scalar relativistic calculation the population of the individual  $5f_{5/2}$  and  $5f_{7/2}$  bands deviates considerably from the statistical ratio of 6:8. This is of course an effect of the spin-orbit interaction since this pushes the  $5f_{5/2}$  band down in energy relative to the  $5f_{7/2}$  band. Actually, as can be seen from Table II, the progressive filling of the  $5f$  states through the series takes place in the  $5f_{5/2}$  band. In Fig. 1 the results of the fully relativistic calculations for the equilibrium volumes of URh<sub>3</sub>, NpRh<sub>3</sub>, PuRh<sub>3</sub>, and AmRh<sub>3</sub> are also

shown. Here we see that for URh<sub>3</sub> the change in volume relative to the scalar relativistic result is small, for NpRh<sub>3</sub> and PuRh<sub>3</sub> it is somewhat larger, and finally it is quite large for AmRh<sub>3</sub>. This brings the theoretical data into quite good agreement with experiment except for AmRh<sub>3</sub>. However for AmRh<sub>3</sub> we have found that a spin-polarized scalar relativistic calculation gives an almost saturated spin-up band, and this reduces the  $5f$  contribution to the chemical bonding to nearly zero. The so calculated equilibrium volume is in rather good agreement with the experimental value (Fig. 1). From this we make the same interpretation as has been previously done for the description of the localization of Am metal, namely that a complete spin polarization mimics the localization and nonbonding properties of the  $5f$  states in Am.<sup>4</sup> Thus the almost fully saturated  $5f$  spin polarization for AmRh<sub>3</sub> is the theoretical evidence for a  $5f^6$  localization in this compound. Similar conclusions can be drawn for CmRh<sub>3</sub>, where again a saturated  $5f$  spin polarization gives an equilibrium volume which agrees fairly well with experiment (Fig. 1).

## V. RELATIVISTIC STONER THEORY

Turning back to the scalar relativistic calculations we observe from Fig. 7 that the value of the DOS at  $E_F$  is low for AcRh<sub>3</sub>, ThRh<sub>3</sub>, PaRh<sub>3</sub>, and URh<sub>3</sub>. On the other hand, for PuRh<sub>3</sub> and AmRh<sub>3</sub> it is quite large and the scalar relativistic calculations actually give a Stoner product<sup>22</sup> that is larger than one for both these systems (Table II). It has been shown, however, that in some cases the spin-orbit interaction can affect the Stoner product quite dramatically. For instance this was found to be the case for  $\delta$ -Pu (Ref. 23) and some Pu compounds.<sup>24</sup> In order to express this quantitatively we have calculated the relativistic Stoner product in two ways. According to Ref. 25 the calculation of the relativistic Stoner product can be performed by including a small uniform fictitious field  $H$  (only acting on the electron spin) to the paramagnetic self-consistent relativistic band calculation. Then a single iteration is done to obtain the induced magnetic moment  $m_{tl}$  on the  $tl$ th orbital ( $t$ =atom type,  $l$ =orbital). From this we define a partial susceptibility  $\chi_{tl}^0 = m_{tl}/H$  and a uniform susceptibility

$$\chi^0 = \sum_{t,l} \chi_{tl}^0. \quad (6)$$

The relativistic Stoner criterion for ferromagnetism can now be formulated as

$$I\chi^0 > 1, \quad (7)$$

where  $I$  is a generalized Stoner parameter

$$I = \sum_{t,l} J_{tl} \left[ \frac{\chi_{tl}^0}{\chi^0} \right]^2 \quad (8)$$

and  $J_{tl}$  is the exchange integral for the  $tl$  state.

We also calculated the Stoner product in an approximate, but analytical, way as suggested in Ref. 26. Here the relativistic Stoner criterion for the onset of ferromagnetism is obtained from the paramagnetic relativistic

tic band-structure calculation and can be written

$$ID_R^T = 1, \quad (9)$$

where  $D_R^T$  is

$$D_R^T = \sum_t n_t \sum_l' D_{tl} + n_A D_R. \quad (10)$$

Here  $n_t$  is the number of atoms of type  $t$  in the Wigner-Seitz cell and  $n_A$  is the number of actinide atoms in this cell. The prime in Eq. (10) indicates that the  $5f$  states are excluded in the summation and  $D_{tl}$  is the  $tl$  partial DOS for all states except the  $5f$ 's. Furthermore  $D_R$  is

$$D_R = \sum_J \sum_{m_j < 0} D_{j,m_j} [(C_+^{j,m_j})^2 - (C_-^{j,m_j})^2]^2, \quad (11)$$

where  $D_{j,m_j}$  is the  $(j, m_j)$ -decomposed DOS for the  $A5f$  states.  $C_+^{j,m_j}$  and  $C_-^{j,m_j}$  are the Clebsch-Gordan coefficients and  $I$  is a generalized Stoner exchange parameter:

$$I = \sum_t n_{tl} \sum_l' \left[ \frac{D_{tl}}{D_R^T} \right]^2 J_{tl} + n_A \left[ \frac{D_R}{D_R^T} \right]^2 J_{Af}. \quad (12)$$

Here  $J_{Af}$  is the exchange integral for the actinide  $f$  states. The basic assumption that leads to these equations is that the splitting between the  $j = \frac{5}{2}$  and  $j = \frac{7}{2}$  states is large, so that interband terms are negligible compared to the diagonal ones. This is reasonable since the spin-orbit coupling is strong for the  $5f$  states in actinide systems. Thus the matrix elements that connect the  $\frac{5}{2}$  and  $\frac{7}{2}$  states can be neglected. In Table II we give the calculated values for the relativistic Stoner product [Eqs. (9)–(12)] for the  $ARh_3$  systems. For  $URh_3$  we also performed a calculation using Eqs. (6)–(8) in order to test the assumptions that lead to the simpler expression in Eqs. (9)–(12). The Stoner products from the two different calculations were found to be almost the same and we conclude that the neglect of the interband matrix elements, keeping only the diagonal ones, is justified. For the heavier compounds in the series this mixing will be even less important. From Table II we find that both  $URh_3$  and  $NpRh_3$  should be paramagnetic. Only for  $PuRh_3$  do we calculate that the relativistic Stoner product is larger than one. Therefore we conclude that  $PuRh_3$  should order magnetically which is in accordance with experiment.

## VI. THE LOCALIZATION IN $UPd_3$

In order to study the influence that ligand states can have on the electronic structure of actinide systems we have performed energy-band calculations for the  $UM_3$  ( $M = {}_{42}\text{Mo}, {}_{43}\text{Tc}, \dots, {}_{47}\text{Ag}$ ) series. These calculations were all done at a fixed volume corresponding to a lattice constant  $a = 4.0 \text{ \AA}$ . Additional calculations where the volume was varied were performed for  $URu_3$ ,  $URh_3$ , and  $UPd_3$ . These three compounds have all been studied experimentally, while the others probably do not form. The calculated equilibrium volume of the  $URu_3$ ,  $URh_3$ , and  $UPd_3$  compounds is shown in Fig. 10 together with

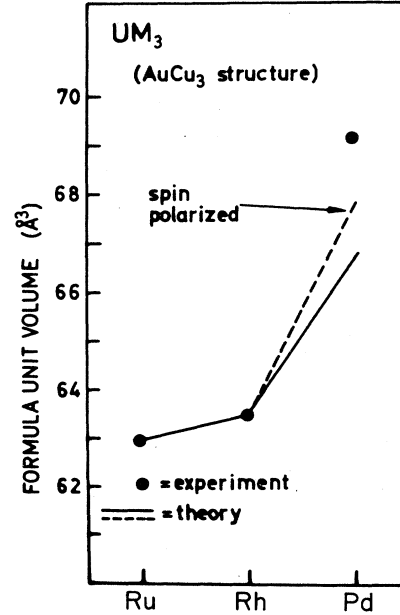


FIG. 10. Experimental and theoretical equilibrium volumes for  $UM_3$  systems ( $M = \text{Ru}, \text{Rh}, \text{and Pd}$ ). All calculations were performed for the  $\text{AuCu}_3$  structure.

the experimental data. Here we notice the good agreement between theory and experiment for  $URu_3$  and  $URh_3$ . However, for  $UPd_3$  the theoretical volume is much too low in comparison to experiment. Neglecting this discrepancy for the moment we notice that the volumes of the  $UM_3$  systems follow the upward part of a parabolic trend. The reason for this is the filling of the  $4d$  states when we add electrons in going from one compound to the next in the series. In order to illustrate this parabolic behavior more clearly we have in Fig. 11 plotted the calculated electronic pressure<sup>13</sup> at a constant

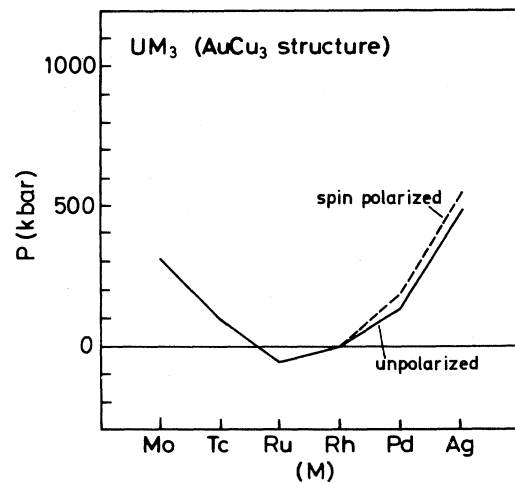


FIG. 11. Calculated pressures for the  $UMo_3$ ,  $UTc_3$ , . . . ,  $UAg_3$  intermetallic systems for a lattice constant  $a = 4.0 \text{ \AA}$ . Also the pressures for the spin-polarized states of  $UPd_3$  and  $UAg_3$  are shown.



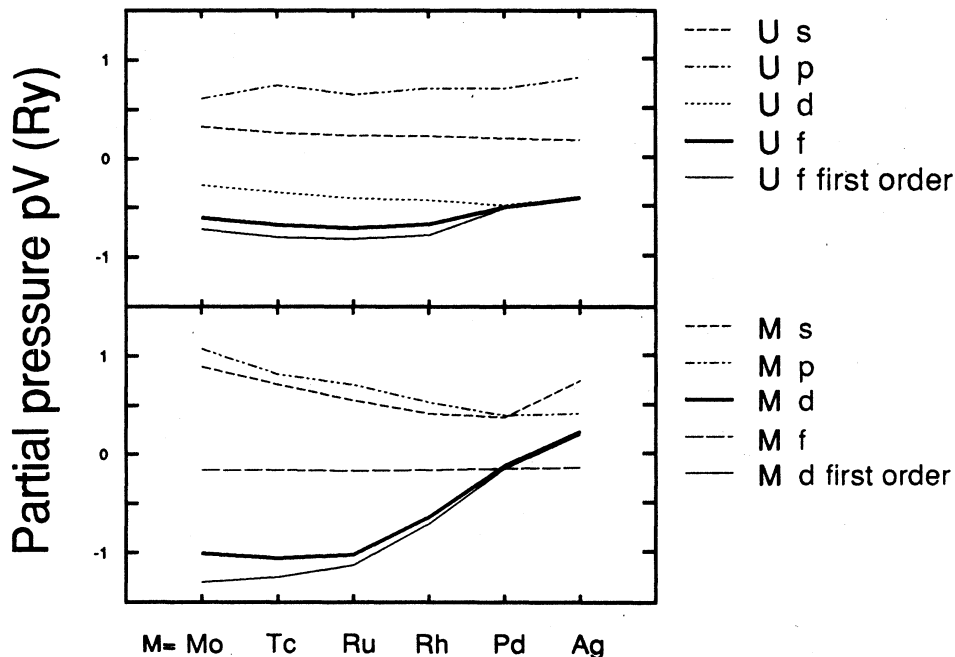


FIG. 12. Calculated partial pressures for the  $UM_3$ ,  $UTc_3, \dots, UAg_3$  intermetallic systems for a lattice constant  $a=4.0 \text{ \AA}$ . Also the approximate first-order pressures [Eq. (1)] for the U  $5f$  and M  $4d$  ( $M=_{42}Mo, _{43}Tc, \dots, _{47}Ag$ ) are given.

volume ( $64.0 \text{ \AA}^3$ ) for the  $UM_3$  systems. Here we see that the minimum in the pressure is located at  $URu_3$  and therefore this system is calculated to have the smallest equilibrium volume. Among the experimentally known compounds this is also the case (Fig. 10).

In Fig. 12 we show the calculated partial pressures at a constant volume for the  $UM_3$  systems and we have also included the  $5f$  and  $4d$  pressure obtained from the simplified expression in Eq. (1). We notice that the parabolic trend of the volumes is mainly due to changes in the  $4d$  partial pressure. We also find that Eq. (1) is rather accurate and compares quite well with the results from the full pressure formula.<sup>13</sup> In Fig. 13 we have separated the contributions to the pressure in Eq. (1) into two parts; the band-center term and the bandwidth term for the  $5f$  and  $4d$  partial pressures. For the  $5f$  partial pressure it is the bandwidth term that dominates whereas for the  $4d$  pres-

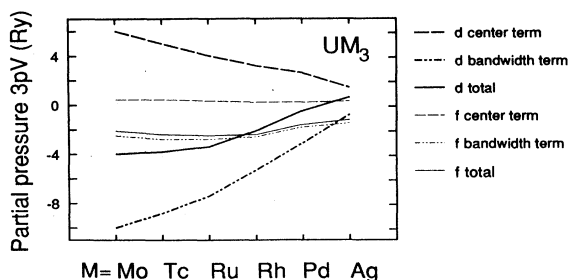


FIG. 13. Band-center and bandwidth terms of the first-order partial pressures of the U  $5f$  and M  $4d$  ( $M=_{42}Mo, _{43}Tc, \dots, _{47}Ag$ ) partial waves.

sure the bandwidth and band-center terms are of almost equal importance but of opposite signs. The net pressure for both the  $4d$  and  $5f$  partial waves is however negative (bonding).

The calculated electron density of states for the  $UM_3$  systems is shown in Fig. 14. Here we notice that the main features of the DOS are composed of bonding and antibonding  $d$  states, as described above, and of  $5f$  states lying at the upper part of the bonding band or between the bonding and antibonding bands. For the earlier systems, up to and including  $URh_3$ , there is strong hybridi-

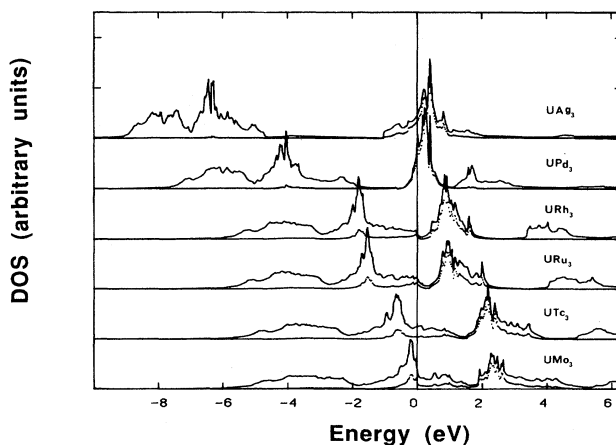


FIG. 14. Density of states for the  $UM_3$ ,  $UTc_3, \dots, UAg_3$  systems calculated for a lattice constant  $a=4.0 \text{ \AA}$ . The low line or dots for each system show the  $5f$  partial density of states. The Fermi level is at zero energy.

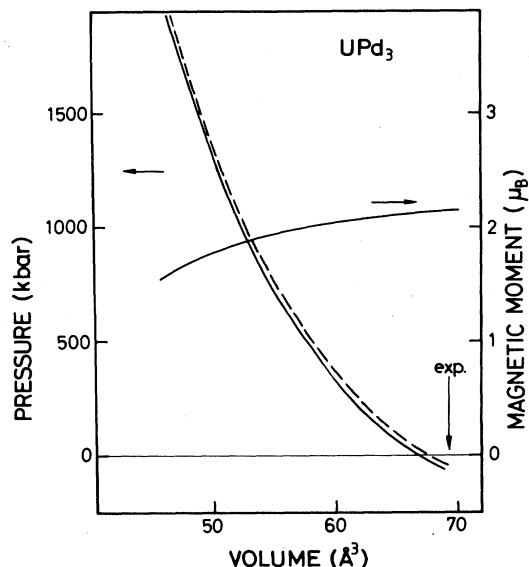


FIG. 15. The paramagnetic and ferromagnetic equation of state for UPd<sub>3</sub> for the AuCu<sub>3</sub> structure. Also given is the total magnetic moment/formula-unit for the ferromagnetic calculation. The experimental volume is marked with a vertical arrow.

zation between the  $5f$  and  $4d$  states and therefore the  $5f$  bandwidth is quite large. However in UPd<sub>3</sub> the  $5f$  band lies in the gap between the bonding and antibonding  $d$  states and accordingly the  $f$ - $d$  hybridization is reduced substantially. This causes the bandwidth to become narrower in UPd<sub>3</sub> than in the earlier UM<sub>3</sub> systems, leading to a high Stoner product in UPd<sub>3</sub>. This suggests that UPd<sub>3</sub> orders magnetically and when allowance for spin polarization is made in the calculations, the ferromagnetic state is indeed found to be stable. In the spin-polarized calculation the spin-down band is almost entirely depleted, leaving practically all the  $5f$  electrons in the spin up band. We argue that this gives theoretical support to the experimental findings that the  $5f$  electrons are localized in UPd<sub>3</sub>. Even though the  $5f$  spin polarization is almost complete there is still in the calculations a substantial contribution of the  $5f$  electrons to the bonding. Therefore, although the ferromagnetic solution gives a larger equilibrium volume than the paramagnetic state, the calculated volume is still far lower than the experimental value (Fig. 10). However, when the  $5f$  pressure is removed artificially, the corresponding volume is in rather good agreement with experimental data.<sup>27</sup> This supports the view that the  $5f$  electrons are localized in UPd<sub>3</sub>.

In Fig. 15 we show the calculated scalar relativistic paramagnetic as well as ferromagnetic equation of state for UPd<sub>3</sub>. Due to the reduced  $5f$  bonding in the ferromagnetic state its equation-of-state curve lies at higher pressures than the corresponding paramagnetic curve

(magnetovolume effect). It is found that the ferromagnetic state is stable even at highly compressed volumes. The  $5f$  spin-down band remains almost empty also at the very lowest volumes shown in Fig. 15. With the interpretation that a completely spin polarized state for the present system corresponds to a  $5f$  localization, we conclude that the localized  $5f$  configuration in UPd<sub>3</sub> is indeed very stable.

## VII. CONCLUSIONS

We have shown that the light  $ARh_3$  systems have delocalized  $5f$  electron behavior but that the heavier systems AmRh<sub>3</sub> and CmRh<sub>3</sub> most likely have localized  $5f$  electrons. We have argued that the dramatic increase in volume between PuRh<sub>3</sub> and AmRh<sub>3</sub> can be understood in terms of a trivalent localized  $5f^6$  configuration in AmRh<sub>3</sub>. We could account for this transition by means of spin-polarized energy band calculations as was previously done for the Am metal,<sup>4</sup> AmN (Brooks, Ref. 19) and the AmIr<sub>2</sub> Laves-phase compound.<sup>25</sup> By using the relativistic generalization of the Stoner theory for the onset of ferromagnetism we could also account for the experimentally known magnetic properties of the  $ARh_3$  systems. In particular we find that NpRh<sub>3</sub> should not order magnetically. This is due to the spin-orbit splitting of the  $5f$  states, since the paramagnetic scalar relativistic calculation for NpRh<sub>3</sub> yields a ground state which is unstable to ferromagnetism. On the other hand, we obtained, in agreement with experiment, that PuRh<sub>3</sub> should be magnetic. More work is needed, however, before we can conclude whether this magnetism is of an itinerant nature or whether the  $5f$  electrons form a localized tetravalent configuration. For the present systems we have shown that the spin-orbit splitting has only a relatively small influence on integrated properties, such as occupation number and electronic pressure.

We have also studied the  $5f$  localization in UPd<sub>3</sub> and found that this system shows an unusually weak hybridization between the  $5f$  states and the ligand  $4d$  states, whereas it is strong for the other UM<sub>3</sub> systems ( $M = Mo, Tc, Ru, Rh$ ). The fundamental reason for this is that the  $5f$  states in UPd<sub>3</sub> are located in the gap between the bonding and antibonding  $d$  states. Even under high compressions the  $5f$  states show very little tendency towards itinerant behavior. We expect a similar tendency to  $5f$  localization for UPt<sub>3</sub>. This is of particular interest in view of the heavy-fermion behavior in UPt<sub>3</sub>.

## ACKNOWLEDGMENTS

Olle Eriksson is grateful to the Bank of Sweden Tercentenary Foundation and Börje Johansson is grateful to the Swedish Natural Research Council for financial support. Valuable discussions with Dr. V. Sechovsky and Dr. L. Havela are acknowledged.

\*Present address: Center for Materials Science, Los Alamos National Laboratory, Los Alamos, New Mexico 87545.

<sup>1</sup>See, for instance, articles in *Handbook on the Physics and Chemistry of the Actinides*, edited by A. J. Freeman and G. H.

Lander (North-Holland, Amsterdam, 1984).

<sup>2</sup>M. S. S. Brooks, H. L. Skriver, and B. Johansson, in Ref. 1, Vol. 1.

<sup>3</sup>J. F. Janak, V. L. Moruzzi, and A. R. Williams, Phys. Rev. B

- 12, 1217 (1975); V. L. Moruzzi, A. R. Williams, and J. F. Janak, *ibid.* **15**, 2854 (1977); C. D. Gelat, H. Ehrenreich, and R. E. Watson, *ibid.* **15**, 1613 (1977); O. K. Andersen, O. Jepsen, and D. Glötzel, in *Highlights in Condensed Matter Theory*, edited by F. Bassani, F. Fumi, and M. P. Tosi (North-Holland, New York, 1985); D. G. Pettifor, *J. Phys. F* **7**, 613 (1977); **7**, 1009 (1977); **8**, 219 (1978).
- <sup>4</sup>H. L. Skriver, O. K. Andersen, and B. Johansson, *Phys. Rev. Lett.* **41**, 42 (1978); **44**, 1230 (1980).
- <sup>5</sup>G. Stewart, *Rev. Mod. Phys.* **56**, 755 (1984); F. Steglich, J. Aarts, C. D. Bredl, W. Lieke, D. Meschede, W. Franz, and H. Schäfer, *Phys. Rev. Lett.* **43**, 1892 (1979); H. R. Ott, M. Rudiger, Z. Fisk, and J. L. Smith, *ibid.* **50**, 1595 (1983).
- <sup>6</sup>D. D. Koelling, B. D. Dunlap, and G. W. Crabtree, *Phys. Rev. B* **31**, 4966 (1984); R. C. Albers, *Phys. Rev. B* **32**, 7646 (1985).
- <sup>7</sup>A. J. Arko, D. D. Koelling, and J. E. Schirber, in Ref. 1 (1985), Vol. 2, p. 175.
- <sup>8</sup>W. Ubachs, A. P. J. van Deursen, A. R. de Vroomen, and A. J. Arko, *Solid State Commun.* **60**, 7 (1986); K. Andres, D. Davidow, P. Dermier, F. Hsu, W. A. Reed, and G. J. Nieuwenhuys, *Solid State Commun.* **38**, 405 (1978).
- <sup>9</sup>J. M. Pountney, J. M. Winterbottom, and I. R. Harris, in *Institute of Physics Conference Series No. 37*, edited by W. D. Corner and B. K. Tanner (Institute of Physics, Bristol, London, 1978), p. 85.
- <sup>10</sup>O. K. Andersen, *Phys. Rev. B* **12**, 3060 (1975); H. L. Skriver, *The LMTO Method* (Springer-Verlag, Berlin, 1984).
- <sup>11</sup>U. von Barth and L. Hedin, *J. Phys. C* **5**, 1629 (1972).
- <sup>12</sup>O. Jepsen and O. K. Andersen, *Solid State Commun.* **1**, 1763 (1971).
- <sup>13</sup>D. G. Pettifor, *Commun. Phys.* **1**, 141 (1976); A. R. Mackintosh and O. K. Andersen, in *Electrons at the Fermi Surface*, edited by M. Springford (Cambridge University, Cambridge, England, 1979).
- <sup>14</sup>L. Vegard, *Z. Phys.* **5**, 17 (1921).
- <sup>15</sup>D. G. Pettifor, *Phys. Rev. Lett.* **42**, 846 (1979).
- <sup>16</sup>B. Johansson, O. Eriksson, M. S. S. Brooks, and H. L. Skriver, *Inorg. Chim. Acta* **140**, 59 (1987).
- <sup>17</sup>O. Eriksson, B. Johansson, M. S. S. Brooks, and H. L. Skriver, *Phys. Rev. B* **39**, 5647 (1989).
- <sup>18</sup>M. B. Brodsky, *Rep. Prog. Phys.* **41**, 1547 (1978).
- <sup>19</sup>O. K. Andersen, H. L. Skriver, H. Nohl, and B. Johansson, *Pure Appl. Chem.* **52**, 93 (1979); M. S. S. Brooks, *J. Phys. F* **14**, 639 (1984); **14**, 653 (1984); **14**, 657 (1984).
- <sup>20</sup>N. E. Christensen, *J. Phys. F* **8**, L51 (1978); C. Godreche, *J. Magn. Magn. Mater.* **29**, 262 (1982); M. S. S. Brooks, *J. Phys. F* **13**, 103 (1983).
- <sup>21</sup>T. Oguchi and A. J. Freeman, *J. Magn. Magn. Mater.* **61**, 1233 (1986).
- <sup>22</sup>S. H. Vosko and J. P. Perdew, *Can. J. Phys.* **53**, 1385 (1975); J. F. Janak, *Phys. Rev. B* **16**, 255 (1977); M. S. S. Brooks, O. Eriksson, and B. Johansson, *Phys. Scr.* **35**, 52 (1987).
- <sup>23</sup>M. S. S. Brooks, B. Johansson, O. Eriksson, and H. L. Skriver, *Physica B+C* **144B**, 1 (1986).
- <sup>24</sup>M. S. S. Brooks, *J. Magn. Magn. Mater.* **63-64**, 649 (1987).
- <sup>25</sup>O. Eriksson, M. S. S. Brooks, and B. Johansson, *J. Phys. (Paris) Colloq.* **49**, C8-695 (1988).
- <sup>26</sup>O. Eriksson, M. S. S. Brooks, and B. Johansson, *Phys. Rev. B* **39**, 13 115 (1989).
- <sup>27</sup>B. Johansson, O. Eriksson, M. S. S. Brooks, and H. L. Skriver, *J. Less-Common Metals* **133**, 25 (1987); O. Eriksson, B. Johansson, M. S. S. Brooks, and H. L. Skriver, *Phys. Rev. B* **38**, 12 858 (1988).